Advances in
Molecular and
Cell Biology

Mathematical modeling of intracellular and intercellular calcium signaling

Jian-Wei Shuai,[a] Suhita Nadkarni,[a] Peter Jung,[a,*] Ann Cornell-Bell[b] and Vickery Trinkaus-Randall[c]

[a]*Department of Physics and Astronomy and Quantitative Biology Institute, Ohio University, Athens, OH 45701, USA*
[*]*Correspondence address: E-mail: jung@helios.phy.ohiou.edu*
[b]*ANSCANS, Ivoryton, CT 06442, USA*
[c]*School of Medicine, Boston University, Boston, MA 02118, USA*

Contents

1. Introduction

The most complex system in the universe is probably the brain. Billions of neurons, interconnected to a large network, perform numerous cognitive and regulatory tasks. Most work on the modeling of brain functions is based on modeling of neuronal networks. The vast majority of cells in the brain, however, are non-neuronal cells or glial cells; about 90% of all brain cells are glial cells. Among several types of glial cells, the astrocytes are known to carry out many important functions, several of them in interactions with neurons.

Astrocytes, in contrast to most neuronal cells, do not fire action potentials due to insufficient Na^+ channel density (Bordeay and Sontheimer, 1998b). Documented exceptions are astrocytomas, where an enhanced expression of Na^+ channels allows the generation of action potentials (Bordeay and Sontheimer, 1998a). Astrocytes do not connect to other astrocytes or neurons via long processes. Therefore, for many years it has

Advances in Molecular and Cell Biology, Vol. 31, pages 689–706

ISBN: 0-444-51451-1

been believed that the role of the glia for brain function is to provide structural and chemical support for the neurons. Such support functions include for example uptake and recycling of neurotransmitters. Although it has been known for a long time that synaptic astrocytes respond with depolarization to neuronal action potentials, this was thought to be a passive response caused by the increased extracellular K^+ concentration. The discovery by Porter and McCarthy (1996), that astrocytes respond to neuronal action potentials by glutamate-mediated activation of metabotropic glutamate receptors, has changed the current thinking about the role of astrocytes dramatically. It is now clear that astrocytes listen to neuronal chatter at the synapses and in turn can modulate neuronal dynamics at the same synapse or over some distance.

As neurons fire, glutamate is released into the synaptic cleft, which is partially lined by the metabotropic glutamate receptors of the synaptic astrocytes. Upon binding of glutamate to the astrocyte, inositol 1,4,5-triphosphate (IP_3) is released into the intracellular space. IP_3 in turn binds to the IP_3 receptor of the endoplasmic reticulum (ER), and Ca^{2+} is released from the ER into the cytosol. As described in more detail below, such Ca^{2+} release can occur in forms of intracellular Ca^{2+} waves. The Ca^{2+} wave can propagate across the cell membrane, through the extracellular space into adjacent astrocytes. As will be discussed below, there are several mechanisms that may be involved in this intercellular signaling. Elevated Ca^{2+} concentrations in synaptic astrocytes generate extracellular glutamate that can modulate the neuronal synapse by generating additional inward currents. This feedback could of course also be inhibitory, if enhanced Ca^{2+} concentrations are activating inhibitory interneurons. In the remainder of this section, we will review recent progress in mathematical modeling of intra- and intercellular Ca^{2+} signaling in general and in the context of astrocytes and their control of synaptic plasticity in particular. We would also like to draw the attention of the reader to another recent review on the same topic by Schuster et al. (2002).

2. Modeling of intracellular Ca^{2+} signaling (IACW)

2.1. Equations used

Ca^{2+} is stored in internal stores, most notably the ER. It can be released into the cytosol through release channels and through passive leakage currents driven by the steep concentration gradient between the ER and the cytosol. The release channels, termed IP_3 receptor channels (IP_3Rs), have been modeled mathematically for more than ten years, and a number of models have been developed. Although the models differ in detail, most models have certain key-elements. Denoting the concentration of Ca^{2+} in the cytosol by c, conservation of Ca^{2+} is expressed by the equation of continuity

$$\frac{\partial c}{\partial t} + \nabla \mathbf{j}_c = \rho(c, \mathbf{x}, t), \tag{1}$$

with $\mathbf{j}_c$ denoting the Ca^{2+} flux density and $\rho(c, \mathbf{x}, t)$ the source density of Ca^{2+}. For not too large gradients in Ca^{2+} concentration Fick's law can be used to relate the flux density to

the Ca^{2+} concentration, i.e.

$$\mathbf{j}_c = -D_{\mathrm{Ca}} \nabla c, \tag{2}$$

with D_{Ca} denoting the diffusion coefficient for calcium. Inserting Eq. (2) into Eq. (1) yields

$$\frac{\partial c}{\partial t} = D_{\mathrm{Ca}} \nabla^2 c + \rho_{\mathrm{Ca}}(c, \mathbf{x}, t). \tag{3}$$

The source density describes the influx of Ca^{2+} into the cytosol per volume and unit time. In the absence of Ca^{2+} entry from the extracellular space, the Ca^{2+} concentration in the cytosol can change due to (i) Ca^{2+} entering from the ER through IP_3Rs, (ii) pump-mediated Ca^{2+} re-uptake by the ER, (iii) leakage of Ca^{2+} from the ER into the cytosol, (iv) Ca^{2+} release from mitochondria, and (v) Ca^{2+} re-uptake by mitochondria, i.e.

$$\rho_{\mathrm{Ca}}(c, \mathbf{x}, t) = -\rho_{\mathrm{pump}} + \rho_{\mathrm{channel}} + \rho_{\mathrm{leak}} - \rho_{\mathrm{mito}}^{\mathrm{in}} + \rho_{\mathrm{mito}}^{\mathrm{out}}. \tag{4}$$

The forms of the source density terms in Eq. (4) differ between the models. The pump term is of Hill-type with a Hill-coefficient of 2 in the two-pool model (Goldbeter et al., 1990)

$$\rho_{\mathrm{pump}} = \frac{k_1 c^2}{k_2^2 + c^2}, \tag{5}$$

the single pool model (Somorgyi and Stucki, 2000; Dupont and Goldbeter, 1993), the De Young–Keizer model (De Young and Keizer, 1992) and the Li–Rinzel model (Li and Rinzel, 1994).

The mathematical form of the source density due to Ca^{2+} release from the ER through IP_3Rs, ρ_{channel}, differs between the models used for the IP_3 receptor. The single and two-pool models use a Hill-form for ρ_{channel}. In the De Young–Keizer model it is assumed that the IP_3 receptor has three independent subunits with three binding sites each: an activating binding site for Ca^{2+}, and inhibiting binding site for Ca^{2+}, and a binding site for IP_3. A subunit is activated if IP_3 is bound and the activating Ca^{2+} binding site is bound. The channel is open, if all three subunits are activated. We denote the state of each channel by a string 'abc' where a, b, and c can assume the values 0 or 1. The first letter indicates occupancy of the IP_3 binding site, the second one the occupancy of the activating Ca^{2+} binding site and the third letter the occupancy of the inactivating Ca^{2+} binding site. A value of '1' indicates that the binding site is occupied while a value '0' indicates that the binding site is unoccupied. The source density ρ_{channel} is thus proportional to the fraction $x_{abc}^3 = x_{110}^3$ of channels with all three subunits bound with IP_3 and Ca^{2+}

$$\rho_{\mathrm{channel}} = v_1 c_1 x_{110}^3 (c_{\mathrm{ER}} - c), \tag{6}$$

where c_{ER} is the Ca^{2+} concentration in the ER. Thus, in this model, the Ca^{2+} flux through the IP_3Rs is driven by the Ca^{2+} concentration difference between the ER and the cytosol, and it is determined by the fraction of channels, x_{110}^3, with all subunits activated. The factor c_1 accounts for the ratio between the volume of the ER and the volume of

the cytosol. The leak current is also driven by the concentration difference between the ER and the cytosol and it is assumed to be of the following form in most models

$$\rho_{\text{leak}} = \nu_2 c_1 (c_{\text{ER}} - c). \tag{7}$$

It is only recently that the effect of Ca^{2+} sequestering by mitochondria has been taken into account for modeling of intracellular Ca^{2+} signaling (Magnus and Keizer, 1997, 1998a,b). The uptake of Ca^{2+} by mitochondria through Ca^{2+} uniporters sets in only when the Ca^{2+} concentration exceeds a threshold. This threshold-like uptake is modeled by a Hill-type expression with a large Hill-coefficient, i.e. (Mahrl et al., 2000)

$$\rho_{\text{mito}}^{\text{in}} = k_{\text{in}} \frac{c^8}{k_2^8 + c^8}, \tag{8}$$

where k_{in} represents the maximum permeability of the Ca^{2+} uniporter and k_2 the half-saturation for Ca^{2+}. In other models, such as the one by Falcke et al. (1999), smaller Hill-coefficients have been used.

Ca^{2+} is released from the mitochondria through Na^+/Ca^+ exchangers and through mitochondrial permeability transition pores. In Mahrl et al. (2000), these two fluxes have been combined into one term, i.e.

$$\rho_{\text{mito}}^{\text{out}} = \left(k_{\text{m}} + k_{\text{out}} \frac{c^2}{K_3^2 + c^2} \right) c_{\text{m}}, \tag{9}$$

where c_{m} is the Ca^{2+} concentration in the mitochondria. Other modelers (Falcke et al., 1999) use a more explicit model that includes the Na^+ concentration in the cytosol and thus links Ca^{2+} signaling directly to transmembrane potentials (see, e.g., Mahrl et al., 1997).

Conservation of total Ca^{2+} requires two additional equations for the Ca^{2+} concentration in the ER, c_{ER}, and the Ca^{2+} concentration in the mitochondria c_{m}, i.e.

$$\frac{\mathrm{d}c_{\text{ER}}}{\mathrm{d}t} = \rho_{\text{Ca}}(c, \mathbf{x}, t) = \rho_{\text{pump}} - \rho_{\text{channel}} - \rho_{\text{leak}} + D_{\text{Ca}}^{(\text{ER})} \nabla^2 c_{\text{ER}}, \tag{10}$$

and

$$\frac{\mathrm{d}c_{\text{m}}}{\mathrm{d}t} = \rho_{\text{mito}}^{\text{in}} - \rho_{\text{mito}}^{\text{out}} + D_{\text{Ca}}^{(\text{mito})} \nabla^2 c_{\text{m}}. \tag{11}$$

The second messenger IP_3 is generated by binding of agonist and can diffuse relatively quickly through the cell, since it is less buffered than Ca^{2+}. The dynamics of IP_3 is thus described by a diffusion equation with a linear decay-term modeling the observed degradation of IP_3, and a production term $\alpha f(\mathbf{x}, t)$ i.e.

$$\frac{\partial c_{\text{IP}}}{\partial t} = \frac{1}{\tau_{\text{IP}}} (c_{\text{IP}}^* - c_{\text{IP}}) + \alpha f(\mathbf{x}, t) + D_{\text{IP}} \nabla^2 c_{\text{IP}}, \tag{12}$$

where c_{IP} is the concentration of IP_3, c_{IP}^* the equilibrium concentration, $1/\tau_{\text{IP}}$ the degradation rate of IP_3 (for recent values, see Wang et al., 1995), and D_{IP} the intracellular diffusion coefficient.

2.2. Deterministic, non-phenomenological modeling

Typically, these models predict Ca^{2+} oscillations or oscillatory spikes, if the concentration of IP_3 is within a certain interval. For the Li–Rinzel model (Li and Rinzel, 1994), e.g., where concentration gradients and mitochondria are neglected, the bifurcation diagram plotted in Fig. 1 is obtained.

For the original parameters in (Li and Rinzel, 1994) one finds a steady state concentration of Ca^{2+} at IP_3 concentrations below 0.345 μM and above 0.642 μM. In between the Ca^{2+} concentration oscillates between the minimum amplitude described by the lower branch in Fig. 1 and the maximum amplitude described by the upper branch.

If the Ca^{2+} concentration is spatially not uniform (the spatial derivatives in the equations above are now taken into account), the Ca^{2+} oscillations are organized in terms of non-linear waves. These waves can have the form of concentric rings (target waves), plane waves and rotating spiral waves. Such waves have been observed to exist in *Xenopus* oocyte (large cells) by Lechleiter and Clapham (1992) and by Lechleiter et al. (1991). Mathematical analysis of these waves have been performed using a two pool model (Dupont and Goldbeter, 1994) or piecewise linear models (Sneyd et al., 1993; Atri et al., 1993). The effect of Ca^{2+} buffers is reviewed, e.g., by Keener and Sneyd (1998). It has been shown by Smith et al. (1998) for cardiac myocytes that to obtain quantitative agreement between simulations and experiments the diffusible indicator dye, which also acts as a buffer, has to be taken into account. This gives rise to yet another pair of non-linear partial differential equations coupled to the equations above. The effect of mitochondria on intracellular Ca^{2+} waves is discussed by Falcke et al. (1999).

2.3. Phenomenological modeling

Phenomenological models that are less demanding in compute time than the stochastic models to be discussed below and also serve well in providing an intuitive picture have

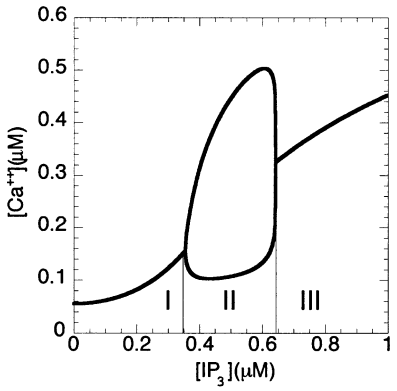

Fig. 1. Bifurcation diagram of the Li–Rinzel model (Li and Rinzel, 1994). The two branches in the interval $0.345 < [IP_3] < 0.642$ μM indicate the minimum and maximum amplitude of the Ca^{2+} oscillations. Below 0.345 μM and above 0.642 μM oscillations are absent.

been used to describe intracellular calcium waves with discrete sources. A simple, but very intuitive model is the fire-and-diffuse model (Keizer et al., 1998a; Dawson et al., 1999). In this one-dimensional model, clustered sources of Ca^{2+} are placed equidistantly on a line. Each source releases a fixed amount of Ca^{2+}, when the Ca^{2+} concentration c exceeds a threshold c_0. When Ca^{2+} is released from a site, it diffuses along the line, increases the Ca^{2+} concentrations at neighboring sites and—depending on the distance between the clusters and the amount of Ca^{2+} being released—can cause Ca^{2+} release at neighboring sites, that in turn can cause release of Ca^{2+} at their neighboring sites, and so on. The model yields analytic values for the speed of the calcium wave.

Another phenomenological model, similar to the fire-and-diffuse model is an excitable cellular-automaton model with discrete release sites (Jung et al., 1998). This model is a two-dimensional array of discrete release sites. Similar to the fire-and-diffuse model, each release site releases a fixed amount of Ca^{2+}, when the local Ca^{2+} concentration exceeds a threshold. According to the model, the released Ca^{2+} diffuses in the intracellular space and approaches instantaneously a stationary, Gaussian profile. In Falcke et al. (2000) and the fire-and-diffuse model, the profiles (although different) are obtained from the reaction-diffusion equations (1)–(12) (with various simplifications) and the one-dimensional diffusion equation, respectively. Qualitatively, the results are similar. If the coupling between the release clusters is small, the waves are abortive. Yet, fluctuations can generate and maintain local patterns spontaneously (Jung and Mayer-Kress, 1995; Jung et al., 1998; Falcke et al., 2000) and aid weak signals in generating a Ca^{2+} response. Characteristic for these noise-sustained patterns are power-law distributed lifetime and size distributions (Jung et al., 1998; Falcke et al., 2000).

2.4. *Stochastic modeling*

2.4.1. *Clustering of Ca^{2+} release channels*

Recently, high-resolution recordings in different types of cells have shed new light on the elementary intracellular Ca^{2+} release events. It has been observed that the Ca^{2+} release channels are spatially organized in clusters with only 20–50 release channels in each cluster, which has a size of about 100 nm. The calcium release through such small clusters is subject to random fluctuations due to thermal open–closed transitions of individual release channels. After Ca^{2+} is released, it rapidly diffuses within the cluster (within a few μs) and out into the cytosol. There, Ca^{2+} is absorbed by buffers and pumped back into the ER and out into the extracellular space (not considered for modeling in this paper) resulting in a spatially and temporally limited event that has been termed calcium puff or spark (Cheng et al., 1999; Callamaras et al., 1998; Melamed-Book et al., 1999; Gonzalez et al., 2000). Ca^{2+} blips arising from the opening of a single release channel have been observed as well (Bootman et al., 1997; Lipp and Niggli, 1998; Sun et al., 1998). Binding of IP_3 activates the calcium release channels and additional binding of Ca^{2+} opens the channels via Ca^{2+} induced Ca^{2+} release (Bezprovanny et al., 1991). Puffs remain spatially restricted at low concentration of IP_3 stimulus, whereas at high levels of IP_3 neighboring clusters become functionally coupled by Ca^{2+} diffusion and Ca^{2+}-induced Ca^{2+} release, so as to support intracellular

Ca^{2+} waves that propagate throughout the cell. Therefore, Ca^{2+} puffs serve as elementary building blocks of intracellular Ca^{2+} waves. Moreover, puffs can arise spontaneously before a wave is initiated and they can act as the triggers to initiate waves (Bootman et al., 1997). During the last three years, mathematical modeling of intracellular Ca^{2+} signaling starting at the elementary Ca^{2+} release of a single cluster have revealed that clustering of the release channels may have profound consequences for the cellular signaling capability (Shuai and Jung, 2003b).

2.4.2. Stochastic models

At the level of a single release cluster, stochastic (i.e., random) effects are dominating. The classification of the Ca^{2+} dynamics in terms of steady state and oscillatory becomes obsolete (Falcke et al., 2000; Shuai and Jung, 2002a,b). The calcium dynamics consists of a strongly random sequence of elementary calcium release events (see Fig. 2). To model intracellular Ca^{2+} dynamics according to a stochastic model of intracellular Ca^{2+} signaling with clustered release channels, the membrane of the ER is modeled as a mosaic of passive and active patches, where the active patches represent the release channel clusters and passive patches contain only pumps and leakage channels. The cell is usually assumed to be flat with a uniform Ca^{2+} concentration across its width in the ER, and another uniform Ca^{2+} concentration in the cytosol to allow two-dimensional modeling. The discreteness and small size of the Ca^{2+} release channels gives rise to novel intracellular Ca^{2+} patterns such as Ca^{2+} puffs, abortive waves (waves that propagate only a short distance and then die out) and tide waves (Falcke et al. 2000; Bär et al., 2001). Similar modeling studies for muscle cells, where the calcium release channels are Ryanodine receptors have been reported by Keizer and Smith (1998). One key issue in Keizer and Smith (1998) and Falcke et al. (2000) is the transition from local calcium sparks to propagating waves, i.e., the spark-to-wave transition. For IP_3 release channels

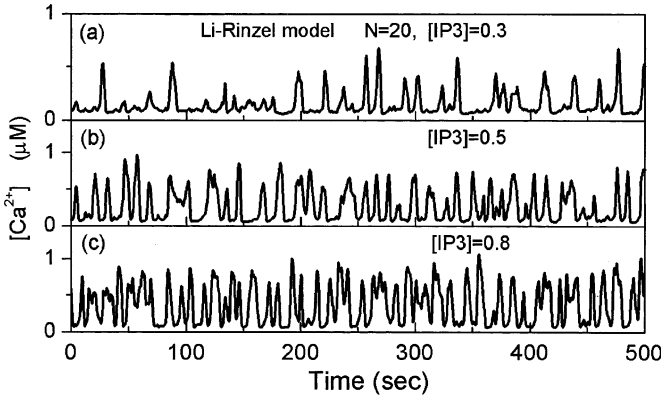

Fig. 2. Calcium released from a single release cluster with 20 release channels at various IP_3 concentrations generated with the stochastic version of the Li–Rinzel Model (Shuai and Jung, 2002a,b). The non-stochastic model predicts Ca^{2+} oscillations between 0.345 and 0.642 μM IP_3 and a steady state Ca^{2+} concentration anywhere else (see Fig. 1). The unit of the IP_3 concentration is μM.

it has been shown in Falcke et al. (2000) that as the intracellular IP_3 concentration is increased, starting from very small sub-threshold values, the calcium patterns change from puffs and abortive waves (sub-threshold) to propagating waves.

Figure 3 shows a sequence of space-time plots (Falcke et al., 2000), where the IP_3 concentration increases from the left panel to the right panel. In the second panel from the left, one can observe abortive waves that—initiated by spontaneous events—propagate through parts of the system and then abort spontaneously. As IP_3 increases, the waves—although still noisy—spread through the entire system and are repetitive, as an oscillatory model (the De Young–Keizer model) has been used.

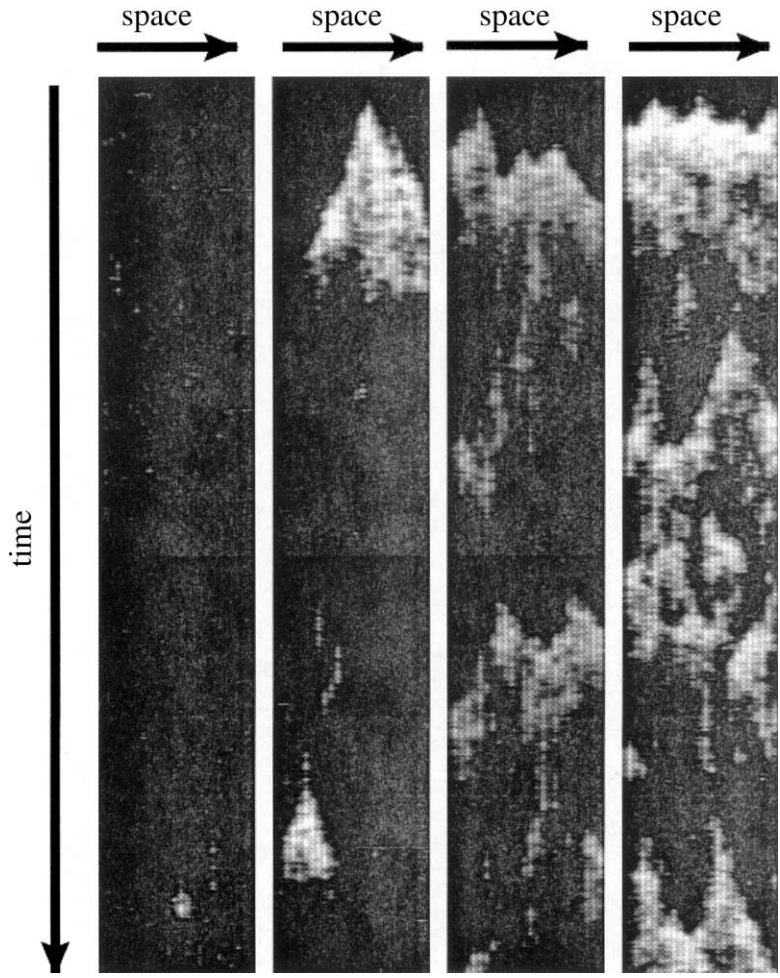

Fig. 3. Space-time plots obtained from a one-dimensional model for intracellular calcium waves with clustered release channels (Falcke et al., 2000). Lighter gray indicates increasing Ca^{2+} concentration. The IP_3 concentration increases from the left panel to the right panel.

A systematic classification of the firing patterns with discrete and stochastic Ca^{2+} release clusters, but neglecting buffers and Ca^{2+} handling by mitochondria (Shuai and Jung, 2003a) is shown in Fig. 4. The 'phase-diagram' of patterns (Ca^{2+} diffusion coefficient versus IP_3 concentration) presented in the figure revealed that essentially all types of observed intracellular Ca^{2+} release patterns could be reconstructed using Eqs. (1)–(12) supplemented with discrete sources of Ca^{2+}. In Fig. 5 snapshots can be seen of different Ca^{2+} transients simulated using this model (Shuai and Jung, 2003a).

2.4.3. Benefit of clustered release channels

Recently it has been suggested that the clustering of the IP_3Rs may enhance Ca^{2+} signaling capability (Shuai and Jung, 2003b). To this end, Eqs. (1)–(12), neglecting effects of mitochondria effects and slow buffers, have been supplemented with spatially discrete distributions of a fixed number of Ca^{2+} release channels with different spatial organization. The stochastic Li–Rinzel model was used to simulate local Ca^{2+} release through IP_3Rs. The concentration of IP_3 was kept below the threshold of Ca^{2+} oscillations observed in Fig. 1. Distributing the release channels homogeneously on the membrane of the ER yielded a cell-averaged low steady-state Ca^{2+} concentration—as one would expect. Clustering the channels at distances such that the total number of release channels is conserved (i.e., larger cluster-distance goes along with larger clusters), it was found that in a certain range of cluster distances (and corresponding sizes) the cell-averaged Ca^{2+} concentrations exhibited strong (almost noise-free) oscillations, coding a weak signal (small IP_3 concentration), that was not coded, when the clusters where homogeneously

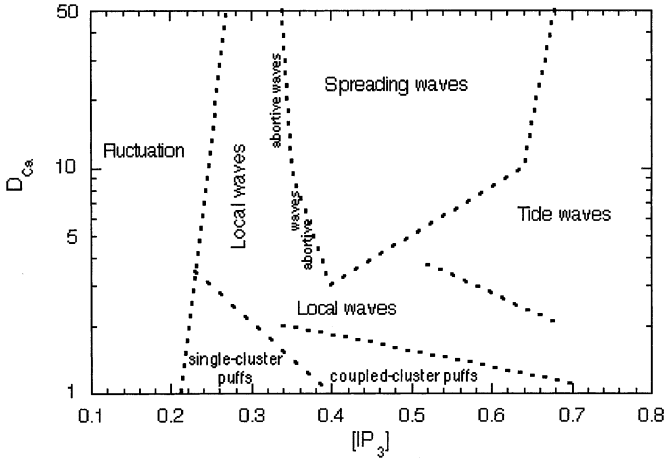

Fig. 4. Phase diagram of intracellular Ca^{2+} patterns from Shuai and Jung (2003a). The diffusion coefficient of Ca^{2+} (D_{Ca}) is indicated in $\mu m^2/s$ and the concentration of IP_3 in μM. The underlying model for the channel fluxes is the spatially extended, stochastic Li–Rinzel model with discrete and clustered Ca^{2+} release channels. The clusters contain 20 IP_3Rs each and are spaced at a distance of 2 μm. The size of the system is 60 $\mu m \times 60$ μm. In the notation used, abortive waves are local, non-propagating but almost propagating waves. Snapshots of the different types of Ca^{2+} transients are shown in Fig. 5.

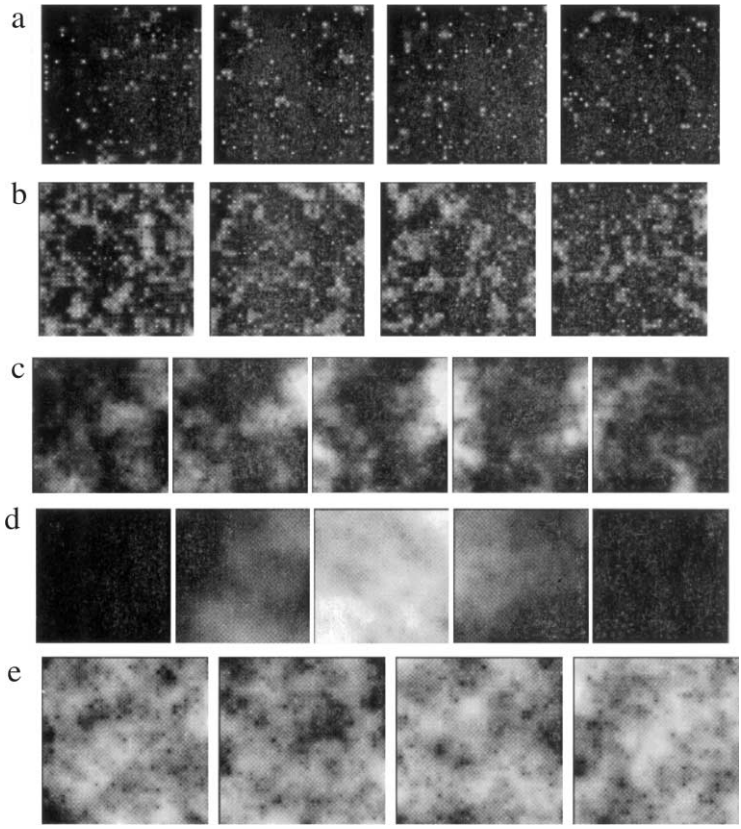

Fig. 5. Snapshots of simulated Ca^{2+} transients as a function of the diffusion coefficient of Ca^{2+} (D_{Ca}) and the IP_3 concentration. Lighter gray indicates increasing Ca^{2+} concentration. The system size is 60×60 μm^2. (a) Ca^{2+} *puffs* at $D = 1$ $\mu m^2/s$ and $[IP_3] = 0.3$ μM at a rate of 1 frame/3 s; (b) *local* Ca^{2+} *waves* at $D = 2$ $\mu m^2/s$ and $[IP_3] = 0.5$ μM at a rate of 1 frame/3 s; (c) *abortive* Ca^{2+} *wave* at $D = 10$ $\mu m^2/s$ and $[IP_3] = 0.35$ μM at a rate of 1 frame/1.4 s; (d) *spreading* Ca^{2+} *wave* at $D = 30$ $\mu m^2/s$ and $[IP_3] = 0.5$ μM at a rate of 1 frame/2.4 s; (e) Ca^{2+} *tide wave* at $D = 10$ $\mu m^2/s$ and $[IP_3] = 0.8$ μM at a rate of 1 frame/2 s. (Data taken from Shuai and Jung, 2003a).

distributed (Shuai and Jung, 2003b). This effect is demonstrated in Fig. 6. The left upper panel shows the cell-averaged Ca^{2+} signal in response to a sub-threshold IP_3 concentration, when 14,400 channels were placed homogeneously at a distance of 0.5 μm over an area of 60 $\mu m \times 60$ μm. The upper panel of the second column in Fig. 6 shows the cell-averaged Ca^{2+} response at cluster distance of 3 μm with a corresponding cluster size of 36 IP_3Rs. The cell-averaged Ca^{2+} signal has now a large amplitude and almost perfect phase coherence, although no parameters other than the geometric distribution of the channels have been changed. The small IP_3 signal is now well encoded in the Ca^{2+} signal. Increasing the cluster distance further to 5 μm with a corresponding cluster size of 100 channels, the cell-averaged Ca^{2+} signal is almost constant with some small fluctuations. Thus the IP_3 signal is not encoded.

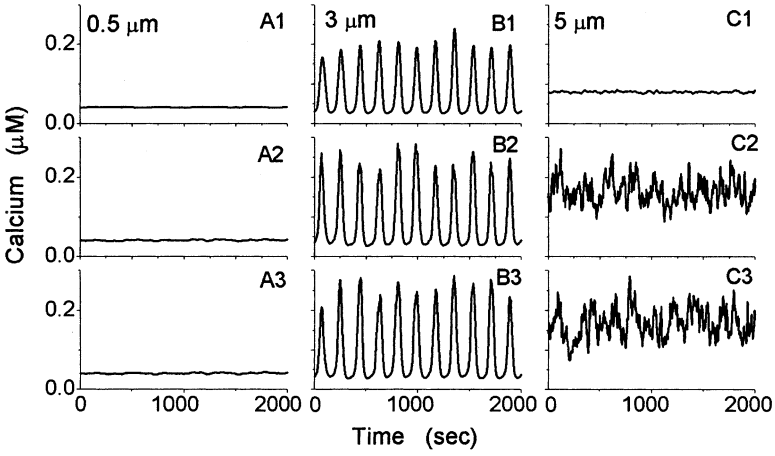

Fig. 6. Ca^{2+} concentrations at two neighboring active sites 0.5 μm apart (A2, A3), 3 μm apart (B2, B3) and 5 μm apart (C2, C3) and the corresponding cell-averaged Ca^{2+} concentrations (A1, B1, C1). The Ca^{2+} diffusion coefficient in the cytosol, $D = 20\ \mu m^2/s$ and $[IP_3] = 0.21\ \mu M$ (Shuai and Jung, 2003b).

Although in most computational studies the clusters of the IP_3Rs are assumed to be organized on a regular grid this is not so in cells. Exceptions are the two recent publications by Falcke (2003a,b) on nucleation of calcium waves and the effects of slow buffers. The clusters are typically close to the cell membrane and are clustered themselves forming 'hot spots'. It remains to be shown whether optimal clustering is robust for these more realistic scenarios.

3. Modeling of intercellular Ca^{2+} signaling (IRCW) in astrocytes

Calcium signals can travel through the cell membrane and propagate through many cells. Intercellular Ca^{2+} waves have been observed in astrocyte cultures (Cornell-Bell et al., 1990; Giaume and Venance, 1998; Charles, 1998), hippocampal slice cultures of mice (Harris-White et al., 1998), cultured glioma cells (Charles et al., 1992), neurons (Charles et al., 1996), and hepatocytes (Combettes et al., 1994; Nathanson and Burgstahler, 1995; Robb-Gaspers and Thomas, 1995; Patel et al., 1999). Although the mechanism for intercellular Ca^{2+} waves (IRCW) is controversial, it is clear that it is different from the mechanism for intracellular Ca^{2+} waves (IACW). There exists a substantial amount of indirect evidence that gap junctions connecting neighboring astrocytes are important for the propagation of IRCW, in that they provide permeability for the intracellular messenger IP_3. If an increased concentration of IP_3 is generated in an astrocyte, it may not only aid in providing intracellular Ca^{2+} via calcium-induced calcium release in the cell in question, but it also may diffuse through gap junction to neighboring astrocytes and contribute to the generation of an intracellular Ca^{2+} response. Such a mechanism has been modeled by Sneyd et al. (1995a,b) and Hofer et al. (2002), with

numerous simplifications. The source density of IP_3 has to be supplemented by the divergence of the flux density through the gap-junctions at the cell-boundaries

$$\nabla \mathbf{j}_{\text{gap}}(\mathbf{x})|_{\text{cell-boundary}}. \tag{13}$$

Assuming Fick's law for the flux through the gap junctions (driven by a gradient in IP_3 concentration), i.e.

$$\mathbf{j}_{\text{gap}} = -D_{\text{gap}} \nabla c_{\text{IP}}, \tag{14}$$

and discretizing the Laplacian in the equation for IP_3 (last term on the right-hand side of Eq. (12)), the additional terms due to the gap junctions are

$$-\frac{D_{\text{gap}}}{\Delta x^2}(c_{\text{IP}}^{n+1} - 2c_{\text{IP}}^{n} + c_{\text{IP}}^{n-1}), \tag{15}$$

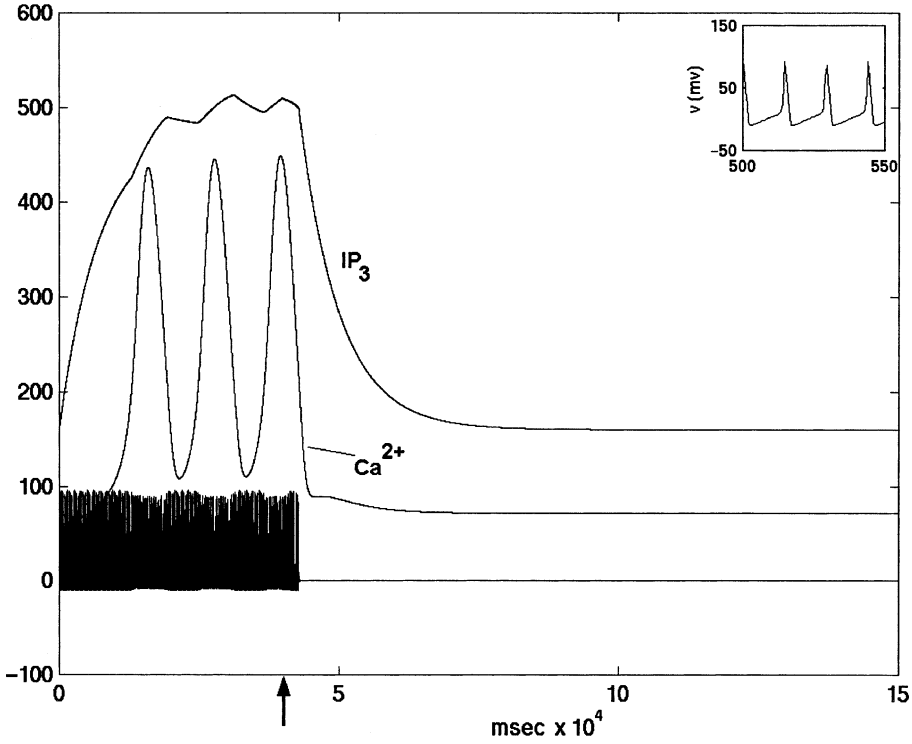

Fig. 7. A DC stimulus is applied to the neuron during the time interval [0–40 s] (end of stimulation interval is indicated by an arrow) at an IP_3 production rate of $\alpha = 0.5$ in the astrocyte. The lowest (dense) curve depicts the neuronal oscillations and an expanded section of it is shown in the inset. As the neuron fires, the concentration of IP_3 in the astrocyte (upper curve) is increasing. If the IP_3 concentration is high enough, intracellular Ca^{2+} oscillations occur. When the stimulus to the neuron is stopped, IP_3 degradation overwhelms the positive feedback into the neuron, and the Ca^{2+} oscillations and the neuronal oscillations disappear.

if the cell-boundary is perpendicular to this spatial direction. Assuming the cell membranes, separating the two cells is located between x_n and x_{n+1}, and a steep gradient of c_{IP} between the cells in comparison to the one within the cells, i.e.

$$c_{\mathrm{IP}}^{n-1} \approx c_{\mathrm{IP}}^{n}, \tag{16}$$

one finds

$$-\frac{D_{\mathrm{gap}}}{\Delta x^2}(c_{\mathrm{IP}}^{n+1} - 2c_{\mathrm{IP}}^{n} + c_{\mathrm{IP}}^{n-1}) \approx \frac{D_{\mathrm{gap}}}{\Delta x^2}(c_{\mathrm{IP}}^{n+1} - c_{\mathrm{IP}}^{n}) \equiv P_{\mathrm{gap}}(c_{\mathrm{IP}}^{n+1} - c_{\mathrm{IP}}^{n})$$

with the gap-junction permeability P_{gap}. Gap junction permeability has not been available in the literature and thus its value needs to be inferred indirectly, e.g., by the propagation distance of a wave. Such a diffusive coupling mechanism leads to a diffusive type of IRCW with a speed that would decrease as it spreads. This prediction is in agreement with

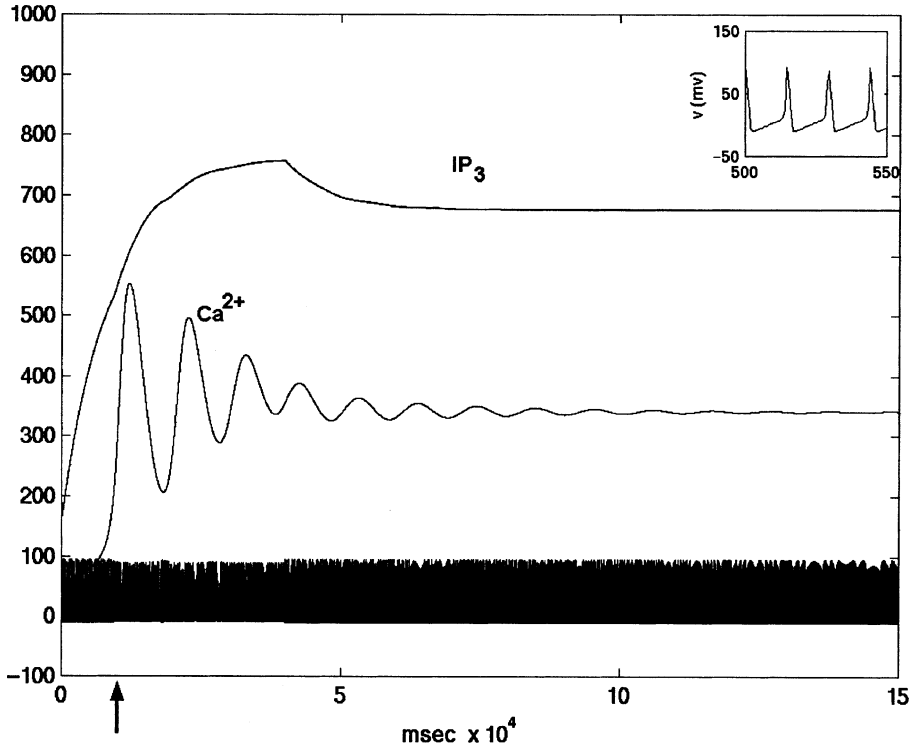

Fig. 8. DC stimulus is applied to the neuron during the time interval [0–40 s] (end of stimulation interval is indicated by an arrow) at the larger IP_3 production rate $\alpha = 0.8$ in the astrocyte. The lowest (dense) curve depicts the neuronal oscillations and an expanded section of it is shown in the inset. As the neuron fires, the concentration of IP_3 in the astrocyte (upper curve) is increasing. If the IP_3 concentration is high enough, intracellular Ca^{2+} oscillations occur. When the stimulus to the neuron is stopped, the production rate of IP_3 (larger than in Fig. 7) overwhelms the degradation and the Ca^{2+} oscillations and neuronal oscillations continue indefinitely.

observations in astrocytes (Sneyd et al., 1995a,b; Harris-White et al., 1998; Jung et al., 1998). It has, however, also been suggested that the diffusion range of IP_3 is not large enough to account for the distance an IRCW is propagating (Giaume and Venance, 1998).

While there is general agreement regarding the role of IP_3 as a messenger (see, however, also chapter by Scemes and Spray), the role of additional extracellular messengers is controversial, and it is a current topic of research. It has been observed that cultured mouse hippocampal astrocytes that were not coupled to other astrocytes by gap junctions, also participate in the IRCW (Hassinger et al., 1996). Using a novel technology to image extracellular ATP it has been reported (Wang et al., 2000) that Ca^{2+} waves triggered by mechanical stimulation are synchronized with a spreading extracellular ATP signal. Based on the propagation range of this signal it has been concluded by Wang et al. (2000) that the signal is regenerative, although it spreads only across a finite distance, i.e., that cells receiving the external ATP signal (by binding of ATP to purinergic receptors), also generate extracellular ATP in response. It has also been speculated that IP_3 traveling through gap junctions may not be the mediator of intercellular Ca^{2+} waves (Wang et al., 2000). This hypothesis is supported by the report by Bushong et al. (2002) that the astrocytes in most of the brain form isolated domains (see chapter by Scemes and Spray) so that only a diffusible extracellular messenger could facilitate direct signals between the cells. However, Arcuino et al. (2002) challenge the hypothesis of a regenerative wave-like ATP signal, concluding that ATP released in response to stimulation from a group of astrocytes diffuses passively through the extracellular space, and Giaume and Venance (1998) find no evidence that extracellular ATP should be involved in the intercellular Ca^{2+} wave. Mathematical modeling that includes extracellular messengers has not been carried through according to our knowledge.

4. Bidirectional coupling between neurons and astrocytes

Recently our group (Nadkarni and Jung, in preparation) has proposed a model for neuronal dynamics, that takes into account the coupling between neurons and astrocytes. The key elements of the model are coupling of Ca^{2+} dynamics in the synaptic astrocytes to neuronal dynamics, described by a conductance-based model. An increased Ca^{2+} concentration in synaptic astrocytes causes an additional inward current in neurons (Parpura and Haydon, 2000), probably due to generation and release of extracellular glutamate from astrocytes. The quantitative relationship between Ca^{2+} concentration in the astrocyte and the additional inward current in the neuron has been fitted by a curve and added to the ionic conductance model. When the neuron fires, it releases glutamate that binds to the metabotropic glutamate receptors on the astrocytes and causes the generation in the astrocyte of IP_3, that in turn contributes to calcium-induced calcium release and an intracellular Ca^{2+} signal. An equation has been set up to simulate the IP_3 concentration (see Eq. (12)), based upon its rates of generation, α, and degradation, $1/\tau_{IP}$ (Wang et al., 1995). The rate of generation of IP_3 in the astrocyte in response to neuronal firing of an action potential is a free parameter. While there is no experimental value available for this rate, we know that it has to be proportional to the density of metabotropic glutamate receptors on the synaptic astrocytes. One of the important conclusions of this study is that the critical value of

the injected current into the neuron (sum of all synaptic inputs) to generate repetitive (periodic) neuronal firing is reduced in the presence of the astrocyte feedback-loop (see Figs. 7 and 8). The IP_3 production rate α, proportional to the density of mGluR is 0.5 s^{-1} in Fig. 7 and 0.8 s^{-1} in Fig. 8 where spontaneous oscillations remain even after the neuronal stimulation is terminated.

As a matter of fact, if the density of metabotropic glutamate receptors on the synaptic astrocytes is large enough (see Fig. 8), oscillations can set off in the absence of external stimulus. In this context it is interesting to note that astrocytes in epileptic foci are known to over-express metabotropic glutamate receptors (Ulas et al., 2000; Aronica et al., 2000; Tang and Lee, 2001).

5. Concluding remarks

We reviewed the recent literature on modeling of intracellular and intercellular calcium waves with focus on brain tissue. We have pointed out the importance of stochastic modeling for intracellular calcium signaling in view of the discreteness of the elementary release events even for cellular signaling capability. Mathematical modeling of intracellular Ca^{2+} signaling of the Ca^{2+} release channel results in enhanced cellular signaling capability in response to weak stimuli with optimal clustering. While intracellular modeling is advanced and capable of reproducing experimental results, modeling of intercellular signals is still patchy and incomplete. Progress in this field requires a better and more complete understanding of the underlying mechanisms that are currently only poorly understood. Bidirectional interaction of astrocytes with neurons can alter the behavior of the neurons. We have reported on a recent study where it has been shown that the feedback from synaptic astrocytes into the same synapse can have the effect of generating spontaneous neuronal oscillations.

Acknowledgements

This material is based upon work supported by the National Science Foundation under Grant No. IBN-0078055.

References

Arcuino, G., Lin, J.H.C., Takano, T., Liu, C., Jiang, L., Gao, Q., Kang, J., Nedergaard, M., 2002. Intercellular calcium signaling mediated by point-source release of ATP. Proc. Natl Acad. Sci. USA 99, 9840–9845.

Aronica, E., van Vliet, E.A., Mayboroda, O.A., Troost, D., da Silva, F.H.L., Gorter, J.A., 2000. Upregulation of metabotrobic glutamate receptor subtype mGluR3 and mGluR5 in reactive astrocytes in a rat model of mesial temporal lobe epilepsy. Eur. J. Neurosci. 12, 2333–2344.

Atri, A., Amundson, J., Clapham, D., Sneyd, J., 1993. A single-pool model for intracellular calcium oscillations and waves in the *Xenopus laevis* oocyte. Biophys. J. 65, 1727–1739.

Bär, M., Falcke, M., Levine, H., Tsimring, L.S., 2000. Discrete stochastic modeling of calcium channel dynamics. Phys. Rev. Lett. 84, 5664–5667.

Bezprovanny, I., Watras, J., Ehrlich, B., 1991. Bell-shaped calcium response curves of Ins(1,4,5) P3- and calcium-gated channels from endoplasmic reticulum of cerebellum. Nature 351, 751–754.

Bootman, M., Niggli, E., Berridge, M., Lipp, P., 1997. Imaging the hierarchical Ca^{2+} signaling system in HeLa cells. J. Physiol. 499, 307–314.

Bordeay, A., Sontheimer, H., 1998a. Electrophysiological properties of human astrocytic tumor cells in situ: enigma of spriking glial cells. J. Neurophysiol. 79, 2782–2793.

Bordeay, A., Sontheimer, H., 1998b. Properties of human glial cells associated with epileptic seizure foci. Epilepsy Res. 32, 286–303.

Bushong, E.A., Martone, M.E., Jones, Y.Z., Ellisman, M.H., 2002. Protoplasmic astrocytes in CA1 stratum radiatum occupy separate anatomical domains. J.Neurosci. 22, 183–192.

Callamaras, N.J., Marchant, S., Sun, X., Parker, I., 1998. Activation and co-ordination of $InsP_3$ mediated elementary Ca^{2+} events during global Ca^{2+} signals in *Xenopus* oocytes. J. Physiol. 509, 81–91.

Charles, A., 1998. Intercellular calcium waves in glia. Glia 24, 39–49.

Charles, A.C., Kodali, S.K., Tyndale, R.F., 1996. Intercellular calcium waves in neurons. Mol. Cell. Neurosci. 7, 337–353.

Charles, A.C., Naus, C.C.G., Zhu, D., Kidder, G.M., Dirksen, E.R., Sanderson, M.J., 1992. Intercellular calcium signaling via gap junctions in glioma cells. J. Cell Biol. 118, 195–201.

Cheng, H., Song, L., Shirokova, N., Gonzalez, A., Lakatta, E.G., Rios, E., Stern, M.D., 1999. Amplitude distribution of calcium sparks in confocal images: theory and studies with an automatic detection method. Biophys. J. 76, 606–617.

Combettes, L., Trans, D., Tordjmann, T., Laurent, M., Berthon, B., Claret, M., 1994. Ca^{2+} mobilizing hormones induce sequentially ordered Ca^{2+} signals in multicellular systems of rat hepathocytes. Biochem. J. 304, 585–594.

Cornell-Bell, A.H., Finkbeiner, S.M., Copper, M.S., Smith, S.J., 1990. Glutamate induces calcium waves in cultured astrocytes: long-range glial signaling. Science 247, 470–473.

Dawson, S.P., Keizer, J., Pearson, J.E., 1999. Fire-diffuse-fire model of dynamics of intracellular calcium waves. Proc. Natl Acad. Sci. USA 96, 6060–6063.

De Young, G.W., Keizer, J., 1992. A single-pool inositol 1,4,5-trisphosphate-receptor-based model for agonist-stimulated oscillations in Ca^{2+} concentration. Proc. Natl Acad. Sci. USA 89, 9895–9899.

Dupont, G., Goldbeter, A., 1993. One-pool model for Ca^{2+} oscillations involving Ca^{2+} and inositol 1,4,5 triphosphate as co-agonist for Ca^{2+} release. Cell Calcium 14, 311–322.

Dupont, G., Goldbeter, A., 1994. Properties of intracellular Ca^{2+} waves generated by a model based on Ca^{2+} induced Ca^{2+} release. Biophys. J. 67, 2191–2204.

Falcke, M., 2003. On the role of stochastic channel behavior in intracellular Ca^{2+} dynamics. Biophys. J. 84, 42–56.

Falcke, M., 2003. Buffers and oscillations in intracellular Ca^{2+} dynamics. Biophys. J. 84, 28–41.

Falcke, M., Hudson, J.L., Camacho, P., Lechleiter, J.D., 1999. Impact of mitochondrial Ca^{2+} cycling on pattern formation and stability. Biophys. J. 77, 37–44.

Falcke, M., Tsimring, L., Levine, H., 2000. Stochastic spreading of intracellular Ca^{2+} release. Phys. Rev. E62, 2636–2643.

Giaume, C., Venance, L., 1998. Intercellular calcium signaling and gap junctionional communication in astrocytes. Glia 24, 50–64.

Goldbeter, A., Dupont, G., Berridge, M.J., 1990. Minimal model for signal-induced Ca^{2+} oscillations and for their frequency encoding through protein phosphorylation. Proc. Natl Acad. Sci. USA 87, 1461–1465.

Gonzalez, A., Kirsch, W.G., Shirokova, N., Pizarro, G., Brum, G., Pessah, I.N., Stern, M.D., Cheng, H., Rios, E., 2000. Involvement of multiple intracellular release channels in calcium sparks of skeletal muscle. Proc. Natl Acad. Sci. USA 97, 4380–4385.

Harris-White, M.E., Zanotti, S.A., Fruatchy, S.A., Charles, A.C., 1998. Spiral intercellular calcium waves in hippocampal slice cultures. J. Neurophysiol. 79, 1045–1052.

Hassinger, T.D., Guthrie, P.B., Atkinson, P.B., Bennet, M.V.L., Kater, S.B., 1996. An external signaling component in propagation of astrocytic calcium waves. Proc. Natl Acad. Sci. USA 93, 13268–13273.

Hofer, T., Venance, L., Giaume, C., 2002. Control and plasticity of intercellular calcium waves in astrocytes: A modeling approach. J. Neurosci., 22, 4850–4859.

Jung, P., Cornell-Bell, A., Madden, K.S., Moss, F., 1998. Noise-induced spiral waves in astrocyte syncytia show evidence of self-organized criticality. J. Neurophysiol. 79, 1098–1101.

Jung, P., Mayer-Kress, G., 1995. Spatiotemporal stochastic resonance in excitable media. Phys. Rev. Lett. 74, 2130–2133.

Keener, J., Sneyd, J., 1998. Mathematical Physiology. Springer, Berlin.

Keizer, J., Smith, G.D., Ponce-Dawson, S., Pearson J.E., 1998a. Saltatory propagation of Ca^{2+} waves by Ca^{2+} sparks. Biophys. J. 75, 595–600.

Keizer, J., Smith, G.D., 1998b. Spark-to-wave transition: saltatory transmission of calcium waves in cardiac myocytes. Biophys. Chem. 72, 87–100.

Lechleiter, J., Clapham, D., 1992. Molecular mechanism on intracellular calcium excitability in *Xenopus laevis* oocytes. Cell 69, 283–294.

Lechleiter, J., Girard, S., Clapham, D., Peralta, E., 1991. Subcellular patterns of calcium release determined by G-protein specific residues of muscarinic receptors. Nature 350, 505–508.

Li, Y., Rinzel, J., 1994. Equations for $InsP_3$ receptor-mediated Ca^{2+} oscillations derived from a detailed kinetic model: a Hodgkin–Huxley like formalism. J. Theor. Biol. 166, 461–473.

Lipp, P., Niggli, E., 1998. Fundamental calcium release events revealed by two-photon excitation photolysis of caged calcium in guinea-pig cardiac myocytes. J. Physiol. 508, 801–809.

Magnus, G., Keizer, J., 1997. Minimal model of β-cell mitochondrial Ca^{2+} handling. Am. J. Physiol. 273, C717–C733.

Magnus, G., Keizer, J., 1998. Model of β-cell mitochondrial calcium handling and electrical activity. I. Cytoplasmic variables. Am. J. Physiol. 274, C1158–C1173.

Magnus, G., Keizer, J., 1998. Model of β-cell mitochondrial calcium handling and electrical activity. II. Mitochondrial variables. Am. J. Physiol. 274, C1174–C1184.

Mahrl, M., Hzberichter, Th., Brumen, M., Heinrich, R., 2000. Complex calcium oscillations and the role of mitochondria and cytosolic proteins. Biosystems 57, 75–86.

Mahrl, M., Schuster, S., Brumen, M., Heinrich, R., 1997. Modeling the interrelation between calcium oscillations and ER membrane potential oscillations. Biophys. Chem. 63, 221–239.

Melamed-Book, N., Kachalsky, S.G., Kaiserman, I., Rahamimoff, R., 1999. Neuronal calcium sparks and intracellular calcium noise. Proc. Natl Acad. Sci. USA 26, 15217–15221.

Nadkarni, S., Jung, P, submitted.

Nathanson, M.H., Burgstahler, A.D., 1995. Coordination of hormone-induced calcium signals in isolated rat hepatocytes couplets; demonstration with confocal microscopy. Mol. Biol. Cell 3, 113–121.

Parpura, V., Haydon, P., 2000. Physiological astrocytic calcium levels stimulate glutamate release to modulate adjacent neurons. PNAS 97, 8629–8634.

Patel, S., Robb-Gaspers, L.D., Stellato, K.A., Shon, M., Thomas, A.P., 1999. Coordination of calcium signaling by endothelia derived nitric oxide in the intact liver. Nat. Cell Biol. 1, 467–471.

Porter, J.T., McCarthy, K.D., 1996. Hippocampal astrocytes in situ respond to glutamate released from synaptic terminals. J. Neurosci. 16, 5073–5081.

Robb-Gaspers, L.D., Thomas, A.P., 1995. Coordination of Ca^{2+} signaling by intercellular propagation of Ca^{2+} waves in the intact liver. J. Biol. Chem. 270, 8102–8107.

Schuster, S., Marhl, M., Hofer, T., 2002. Modelling of simple and complex calcium oscillations—from single-cell responses to intercellular signaling. Eur. J. Biochem. 269, 1333–1355.

Shuai, J.W., Jung, P., 2002a. Optimal intracellular calcium signaling. Phys. Rev. Lett. 88, 068102.

Shuai, J.W., Jung, P., 2002b. Stochastic properties of Ca^{2+} release of inositol 1,4,5-trisphosphate receptor clusters. Biophys. J. 83, 87–97.

Shuai, J.W., Jung, P., 2003. Selection of intracellular calcium patterns in a model with clustered Ca^{2+} release channels. Phys. Rev. E 67, article #031905.

Shuai, J.W., Jung, P., 2003a. Phys. Rev. E (in press).

Shuai, J.W., Jung, P., 2003b. Optimal ion channel clustering for intracellular calcium signaling. Proc. Natl Acad. Sci. USA 100, 506–510.

Smith, G.D., Keizer, J.E., Stern, M.D., Lederer, W.J., Cheng, H., 1998. A simple numerical model of calcium spark formation and detection in cardiac myocytes. Biophys. J. 75, 15–32.

Sneyd, J., Girard, S., Clapham, D., 1993. Calcium wave propagation by calcium-induced calcium release: an unusual excitable system. Bull. Math. Biol. 55, 315–344.

Sneyd, J., Keizer, J., Sanderson, M.J., 1995. Mechanism of calcium oscillations and waves: a quantitative analysis. FASEB J. 9, 1463–1472.

Sneyd, J., Wetton, B.T.R., Charles, A.C., 1995. Intercellular calcium waves mediated by diffusion of inositol thiphosphate: a two dimensional model. Am. J. Physiol. 268, C1537–C1545.

Somorgyi, R., Stucki, J.W., 2000. Hormone-induced calcium oscillations in liver cells can be explained by a simple one pool model. J. Biol. Chem. 266, 11068–11077.

Sun, X.N., Callamaras, N.J., Marchant, J.S., Parker, I., 1998. A continuum of $InsP^3$-mediated elementary Ca^{2+} signaling events in *Xenopus* oocytes. J. Physiol. 509, 67–80.

Tang, F.R., Lee, W.L., 2001. Expression of the group II and III metabotropic glutatmate receptors in the hippocampus of patients with mesial temporal lobe epilepsy. J. Neurocytol. 30, 137–143.

Ulas, J., Satou, T., Ivins, J.P., Kesslak, C.W., Balazs, R., 2000. Expression of metabotropic gluatamet receptor 5 Is increased in astrocytes after kainate-induced epileptic seizures. Glia 30, 352–361.

Wang, S.S.H., Alousi, A.A., Thompson, S.H., 1995. The life time of inositol 1,4,5-triphosphate in single cells. J. Gen. Physiol. 105, 149–171.

Wang, Z., Haydin, P.G., Yeung, E.S., 2000. Direct observation of calcium-independent intercellular ATP signaling in astrocytes. Anal. Chem. 72, 2001–2007.